

Testing formation mechanisms of the Milky Way’s thick disc with RAVE

Michelle L. Wilson^{1*}, Amina Helmi^{2†}, Heather L. Morrison¹, Maarten A. Breddels², O. Bienaymé³, J. Binney⁴, J. Bland-Hawthorn⁵, R. Campbell^{6,7}, K.C. Freeman⁸, J.P. Fulbright⁹, B.K. Gibson¹⁰, G. Gilmore¹¹, E.K. Grebel¹², U. Munari¹³, J.F. Navarro¹⁴, Q.A. Parker^{5,7}, W. Reid⁷, G. Seabroke¹⁵, A. Siebert³, A. Siviero^{12,13}, M. Steinmetz⁶, M.E.K. Williams⁶, R.F.G. Wyse⁹, T. Zwitter¹⁶

¹Department of Astronomy, Case Western University, Cleveland, OH, 44106, USA

²Kapteyn Astronomical Institute, P.O. Box 800, Groningen, The Netherlands

³Université de Strasbourg, Observatoire Astronomique, Strasbourg, France

⁴Rudolf Peierls Centre for Theoretical Physics, Oxford

⁵Anglo-Australian Observatory, Sydney, Australia

⁶Astrophysikalisches Institut Potsdam, Potsdam, Germany

⁷Macquary University, Sydney, Australia

⁸Australian National University, Canberra, Australia

⁹Johns Hopkins University, Baltimore, MD, USA

¹⁰University of Central Lancashire, Preston

¹¹Institute of Astronomy, Cambridge

¹²Astronomisches Rechen-Institut, Zentrum für Astronomie der Universität Heidelberg, Heidelberg, Germany

¹³INAF Astronomical Observatory of Padova, 36012 Asiago, Italy

¹⁴University of Victoria, Victoria, Canada

¹⁵Mullard Space Science Laboratory, University College London, Holmbury St Mary, Dorking, RH5 6NT, UK

¹⁶Faculty of Mathematics and Physics, University of Ljubljana, Ljubljana, Slovenia

15 October 2018

ABSTRACT

We study the eccentricity distribution of a thick disc sample of stars observed in the Radial Velocity Experiment (RAVE) and compare it to that expected in four simulations of thick disc formation in the literature (accretion of satellites, heating of a primordial thin disc during a merger, radial migration, and gas-rich mergers), as compiled by Sales et al. (2009). We find that the distribution of our sample is peaked at low eccentricities and falls off smoothly and rather steeply to high eccentricities. This distribution is fairly robust to changes in distances, thin disc contamination, and the particular thick disc sample used. Our results are inconsistent with what is expected for the pure accretion simulation, since we find that the dynamics of local thick disc stars implies that the majority must have formed *in situ*. Of the remaining models explored, the eccentricity distribution of our stars appears to be most consistent with the gas-rich merger case.

Key words: Galaxy: disc - solar neighbourhood – Galaxy: formation – Galaxy: structure

1 INTRODUCTION

The thick disc has been a known component of the Milky Way for over 20 years (Yoshii 1982; Gilmore & Reid

1983). Analogous components have been identified in external galaxies, revealing that thick discs may be quite generic features (Burstein 1979; van der Kruit & Searle 1981; Yoachim & Dalcanton 2006). Most of the thick disc formation scenarios that have been proposed fall into one of the following four categories: accretion, heating via a mi-

* E-mail: mlw36@case.edu

† E-mail: ahelmi@astro.rug.nl

nor merger, radial migration, and intense star formation in a gas-rich turbulent environment.

In the accretion model, satellites infall on coplanar orbits and form the thick disc as they are disrupted and incorporated into the main galaxy; in this case, the thick disc would thus consist of stars originating largely (more than 70 per cent in the simulations of Abadi et al. 2003) in several disrupted satellites.

The most often discussed scenario for the formation of a thick disc is the accretion of a massive satellite by a pre-existing disc galaxy, which is thus heated dynamically. The resulting thick disc is mainly made from stars that originated in the primary galaxy’s primordial thin disc rather than the merging satellite. For example in the simulations by Villalobos & Helmi (2009), 10 to 20 per cent of the stars in the remnant thick disc at the “Solar” radius are accreted.

During a turbulent gas-rich phase, stars may also form in a thick disc. This can happen in massive clumps in a rotationally supported component, as in the simulations of Bournaud et al. (2009), but also during gas-rich mergers as shown by Brook et al. (2004). In the latter case, the resulting thick disc stars would have been formed *in situ* and with relatively hot kinematics.

Merging events of any variety might be unnecessary to explain the phenomena, however. Stars may migrate radially from the inner parts of a galaxy to the outer regions due to resonant interactions with spiral arms (Sellwood & Binney 2002) and a bar (Minchev & Famaey 2009). Although the migration process itself does not heat the disc, a greater vertical velocity in the higher surface brightness central regions results in larger heights above the plane being reached in the outer regions where the surface brightness is lower (Kregel, van der Kruit, & Freeman 2005). Migration can thus result in the formation of a thick disc from thin disc stars without any external stimulus (Roškar et al. 2008; Schönrich & Binney 2009).

Recently, Sales et al. (2009) suggested a dynamical test that could differentiate between the formation models and be applied to data to disentangle which is the most likely to have occurred in our galaxy: they propose using the eccentricities of thick disc stars as a discriminant, as populations formed *in situ* are likely to move on low eccentricity orbits, while those accreted can have any eccentricity, but will typically be biased towards higher values. As kinematic data for thick disc stars become available from surveys such as the Radial Velocity Experiment (RAVE Steinmetz et al. 2006), SEGUE (Yanny et al. 2009), and eventually *Gaia*, we can apply these tests to see what they can reveal about thick disc formation.

In this paper, we investigate and constrain the dynamics of a sample of Milky Way thick disc stars and compare the resulting eccentricity distribution to what is expected for the above four models. We use data from the RAVE survey and distances calculated in the manner of Breddels et al. (2010) but with modifications described in Section 2. In Section 3 we derive the eccentricity distribution of the stars and in Section 4 we then examine this in light of the accretion, heating, merger, and migration simulations discussed in Sales et al. (2009).

2 DATA

2.1 The RAVE survey

RAVE¹ measures radial velocities and stellar atmospheric parameters from spectra using the 6dF multi-object spectrometer on the Anglo-Australian Observatory’s 1.2 m UK Schmidt Telescope. The survey looks in the Ca-triplet region (8410-8795 Å), has a resolution of ~ 7500 , and is magnitude limited. The targets chosen are southern hemisphere stars taken from the Tycho-2, SuperCOSMOS and DENIS surveys with I-band magnitudes between 9 and 13. The average internal errors in radial velocity (RV) are $\sim 2 \text{ km s}^{-1}$, and the approximate RV offset between RAVE and the literature is smaller than $\sim 1 \text{ km s}^{-1}$. The catalogue also includes 2MASS photometry and proper motions from Starnet 2.0, Tycho-2, SuperCOSMOS, and UCAC2. For more information about RAVE, see Zwitter et al. (2008).

2.2 Distances

Distances were calculated along the lines of Breddels et al. (2010). We briefly sketch the method here and refer the reader to Breddels et al. (2010) for more details.

The stars are fit using the Y^2 (Yonsei-Yale) isochrones (Demarque et al. 2004) and their measured characteristics. The measured quantities of the stars (T_{eff} , $\log(g)$, $[M/H]$, J , and $J - K_s$) from the RAVE pipeline (Zwitter et al. 2008) and 2MASS are used to minimise the χ^2 statistic to find the closest model star for each observed star. Then, the errors of the observed quantities, which are assumed to be Gaussian, are utilised in a Monte Carlo simulation, from which the absolute magnitude and its error are determined from the resulting probability distribution function. Stars for which none of the isochrones provide adequate matches are discarded. Since the Y^2 isochrones do not extend past the RGB tip, clump stars may result in poor fits; in addition we have explicitly removed the clump stars that should remain in the data set (see Section 2.3).

The effectiveness of this distance method was examined in detail in Breddels et al. (2010), but the main points will be mentioned here. Comparison to main sequence stars observed by HIPPARCOS showed good agreement in the measured parallaxes. To test the distances for giants, Breddels et al. (2010) used the members of M67, an old open cluster. The mean of the calculated distances was 1.48 ± 0.36 kpc, compared to 0.78 kpc from VandenBerg et al. (2007). This discrepancy is related to the fact that when age is left as a variable, stars on the giant branch are sometimes fit better by (unrealistically) younger isochrones. However, when using the 4 Gyr isochrones, which corresponds to the accepted age for the cluster, the distances agreed with those in the literature within error (see Figure 1).

This has motivated us to calculate distances for all stars setting the age at 10 Gyr, which is the characteristic age of the thick disc (Edvardsson et al. 1993). This implies that our method will assign incorrect distances to younger thin disc stars, but since younger giant branches are brighter than older ones, this assumption results in the assigned distances

¹ We use the 30 August 2008 internal data release, which consists of 135,338 stars.

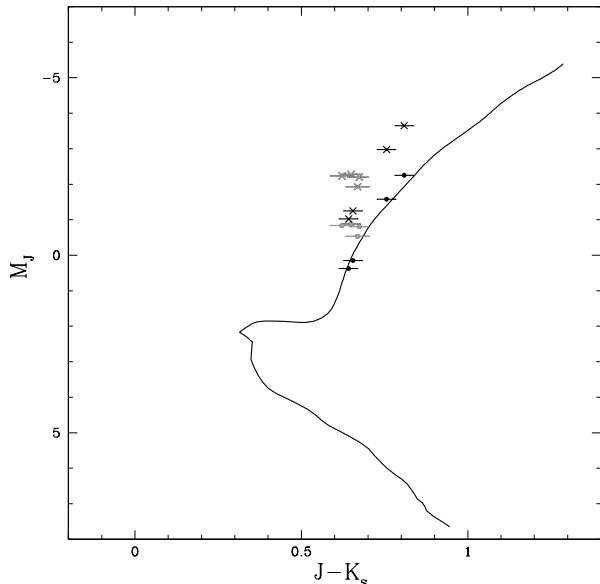


Figure 1. The theoretical solar metallicity, 4 Gyr isochrone with the CMD of M67 giants. Points with crosses are the M67 stars transformed to absolute magnitudes using the Breddels et al. (2010) distance calculated after excluding the clump stars of 1.48 kpc; filled points use the distance of 0.78 kpc calculated assuming an age of 4 Gyr. Gray points are stars identified as belonging to the red clump.

to younger stars being slightly smaller than they actually are. As discussed in Sec. 2.3, we will be selecting stars with $1 \text{ kpc} \leq |z| \leq 3 \text{ kpc}$, so as to isolate a thick disc sample. The consequence of using the “wrong” isochrone for young stars is to reduce their $|z|$ and to move many from lower $|z|$ out of our sample rather than scattering thin disc stars up into it. Even so, we investigated what effect that would have on the distances and the level of thin disc contamination more quantitatively in Section 3.2.2.

2.3 Sample selection

We first cleaned the data set by discarding any stars with distance errors > 40 per cent, proper motion errors in either RA or DEC $> 10 \text{ mas/yr}$, or radial velocity errors $> 5 \text{ km s}^{-1}$. Once the age was set at 10 Gyr, the clump stars were not fit well by any of the isochrones, so most of them should have been discarded on that basis. To ensure all clump stars were indeed removed, however, we threw out stars with $\log(g) > 1.5$ and $J - K_s < 0.75$.

In order to isolate a sample of thick disc stars, we chose the remaining stars with $|z|$ between 1 and 3 thick disc scale-heights, which corresponds to the range 1 – 3 kpc (Veltz et al. 2008). The decision to make our thick disc selection based only on $|z|$ rather than including a metallicity criterion was motivated partly by uncertainties in the

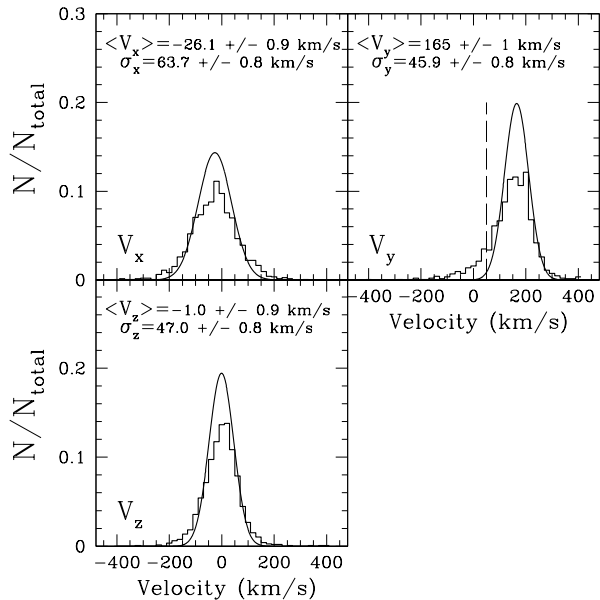


Figure 2. Velocity distributions of our thick disc sample (1273 stars) computed in a right-handed reference frame at rest with respect to the Galactic centre. Mean velocity values and dispersions, calculated using robust estimation, for each component are given in each panel. Stars to the left of the dashed line in V_y were discarded when calculating the means and dispersions.

RAVE’s metallicity pipeline², but also because this mimics more closely the selection by Sales et al. (2009). We further clipped our sample, discarding all stars with $V_y < 50 \text{ km s}^{-1}$ to minimise contamination from the halo, and including only stars within a heliocentric cylinder with a radius of 3 kpc so the data was in a form best suited for comparison with the eccentricity distributions of models as illustrated by Sales et al. (2009). The final sample consisted of 1273 stars. The velocity distributions are given in Figure 2. The velocity dispersions are generally consistent with the literature values, especially in V_x , while those in V_y and V_z are slightly higher by approximately $6 - 8 \text{ km s}^{-1}$ (Sparke & Gallagher 2006).

3 RESULTS

3.1 Eccentricity distribution

To calculate the eccentricities of the RAVE stars in our thick disc sample we integrated their orbits in a Galactic potential. This consisted of a Miyamoto & Nagai (1975) disc, a Hernquist (1990a) bulge and a spherical logarithmic halo. In this model, the characteristic parameters used were $M_{\text{disc}} = 8.0 \times 10^{10}$, $M_{\text{bulge}} = 2.5 \times 10^{10}$, $v_{\text{halo}}^2 = 27000.0$, $a = 6.5$, $b = 0.26$, $c = 0.7$, and $d = 12.0$, with masses in M_{\odot} , velocities in km s^{-1} , and lengths in kpc, which produce a

² For completeness, we have tested that our results do not change appreciably when we focus only on the subset of stars with high S/N spectra which according to their $[M/H]$ belong to the thick disc.

circular velocity of $\sim 220 \text{ km s}^{-1}$ at 8 kpc from the Galactic centre. The eccentricities of the stars were defined as $(r_{\text{apo}} - r_{\text{peri}})/(r_{\text{apo}} + r_{\text{peri}})$, where r_{apo} (r_{peri}) is the maximum (minimum) distance reached by the star in its orbit. Figure 3 shows the eccentricity distribution obtained for our sample. The main features of this distribution are an asymmetric peak at a fairly low eccentricity value with a relatively (though not entirely) smooth falloff towards higher eccentricities. This peak at low eccentricity suggests that the thick disc was formed primarily *in situ* (see Section 4.2).

3.2 Robustness of the eccentricity distribution

3.2.1 Systematic errors

We expect that the largest contribution to systematic errors would be due to the distances. Distance overestimation would result in larger heliocentric velocities, because the observed proper motions would be placed at larger distances. Thus, the distance overestimation should result in a peak at a higher eccentricity than more accurate distances would reveal, not a peak at lower eccentricities, suggesting that the calculated distribution would not likely be a result of distance overestimation. On the other hand, distance underestimation should result in smaller heliocentric velocities and more circular orbits, and thus could cause an artificially strong peak at low eccentricity.

To explore more quantitatively how errors in distance could affect the final eccentricity distribution, we calculated eccentricities for the thick disc sample using distances that were larger and smaller by 20 percent. This value was chosen because nearly all the stars in the sample had distance errors smaller than 20 per cent, with a peak at 10 percent, making this figure conservative. As Figure 3 shows, the distribution with smaller distances has a slightly higher peak at a slightly smaller eccentricity than the original distribution, and that with larger distances has a slightly lower peak at a slightly larger eccentricity, as expected. However, both distributions remain reasonably close to the original one, which suggests that a systematic distance error of 20 percent would not result in a substantial change in the thick disc's eccentricity distribution. We have found that even with up to 40 percent larger distances, the peak in eccentricity remains below 0.4 and the generally triangular shape does not change.

We have also tested how our proper motion errors affect the eccentricity distribution. We found that the main effect is to slightly lower the amplitude of the peak at eccentricity ~ 0.2 and to marginally increase the number of stars with high eccentricity. Therefore we conclude that the shape of the eccentricity distribution is generally robust to the estimated uncertainties in our observables.

3.2.2 Investigation of possible thin disc contamination

Since the thin disc characteristically has stars on fairly circular orbits, there is a possibility that the peak at low eccentricity is caused partially by thin disc contamination in our sample.

To give a quantitative estimate of this contamination, we formulated a simple model. Using the Padova isochrones

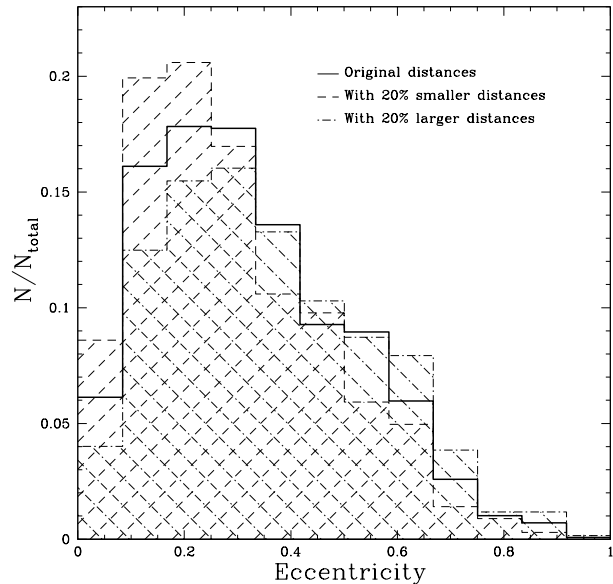


Figure 3. Eccentricity distribution of the thick disc sample using the original distances (1273 stars, solid histogram) and distances that are 20 percent smaller (1350 stars, dashed histogram) and larger (1204 stars, dashed-dotted histogram). The differing numbers of stars are a result of discarding stars with low rotational velocity, since this number depends on what distance is assumed.

and the Chabrier (2001) initial mass function (IMF), we generated two samples of stars. A thin disc population was created from a solar metallicity, 5 Gyr isochrone, and a thick disc population was created from an isochrone with $[\text{Fe}/\text{H}] = -0.6$ dex and an age of 10 Gyr. The relative fraction of thin to thick disc stars $f_{\text{thin2thick}}$ was calculated using the expression

$$f_{\text{thin2thick}} = f_{\text{norm}} * e^{-|z|/z_{\text{thin}} + |z|/z_{\text{thick}}},$$

where f_{norm} is the relative fraction at the Sun, and z_{thin} and z_{thick} the thin and thick disc scale heights respectively. We assumed $z_{\text{thin}} = 225 \text{ pc}$ and $z_{\text{thick}} = 1048 \text{ pc}$, as estimated by Veltz et al. (2008) for the RAVE sample. The local normalisation f_{norm} was calculated using the Veltz et al. (2008) ratio of thin to thick disc dwarfs and the Padova isochrones to determine the fraction of dwarfs for the thin and thick disc samples. We assigned z from 1050 pc to 2950 pc in increments of 100 pc and selected the model stars that would have been observed by RAVE ($9 < I < 13$). To synthesise the effect of calculating distances assuming an age of 10 Gyr on the younger thin disc population, we found the absolute magnitude on the giant branch that would have been assigned to each thin disc star using a solar metallicity, 10 Gyr isochrone based on their effective temperatures. New distances were calculated for the stars with the new absolute magnitudes and the original apparent magnitudes and then re-binned based on these new distances.

Ratios of the number of observed thin disc stars (both using the 5 and 10 Gyr ages) to observed thick disc stars were then computed for each bin in distance and overall. In the lowest z bin, the thin disc contamination was as large as 30 percent, but it dropped to about 10 percent for the 10

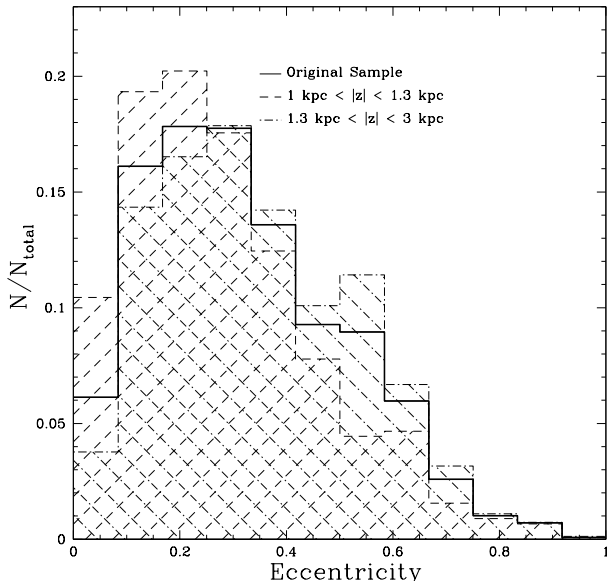


Figure 4. Eccentricity distributions of the original sample (solid), the subsample of stars with $1 \text{ kpc} < |z| < 1.3 \text{ kpc}$ (dashed histogram, 450 stars), and the subsample with $1.3 \text{ kpc} < |z| < 3 \text{ kpc}$ (dashed-dotted histogram, 823 stars).

Gyr thin disc by $z = 1250 \text{ pc}$ and by $z = 1350 \text{ pc}$ for the 5 Gyr thin disc. Since the effect of calculating the distances of younger stars with 10 Gyr isochrones is to underestimate their distances, the thin disc contamination was lower at most z intervals for the 10 Gyr thin disc ratios, since moving the stars down in z took many out of the z range considered. The overall thin disc contamination for the 5 and 10 Gyr thin discs were, respectively, 4.7 and 3.1 percent.

Since those ratios suggest that there could be significant contamination in the portion of our sample that is closest to the plane of the disc, we took our thick disc sample and divided it into a low $|z|$ and a higher $|z|$ portions to see how robust the shape of the eccentricity distribution was to thin disc contamination. Two separate trials were performed. In the first, the division was placed at $|z| = 1.3 \text{ kpc}$, because the simple model suggests that the contamination levels have dropped below 10 percent by that height when the stars all were assigned 10 Gyr ages, as is the case for the data set. The resulting eccentricity distributions for each subsection were then calculated and are plotted in Figure 4. The distribution of the lower $|z|$ portion is strongly peaked at low eccentricity with fewer stars at higher eccentricities, which would be expected for a sample contaminated by thin disc stars, which have predominantly circular orbits. The higher $|z|$ sample retained the roughly triangular shape of the original sample, however. The peak did shift slightly to higher eccentricity, but not significantly.

We also performed another trial and cut the sample at $|z| = 1.5 \text{ kpc}$. The resulting eccentricity distributions of the two subsamples were similar to those of the first trial. The distribution of stars in the higher $|z|$ subsample was lumpier, since there were fewer stars in it, and a slightly increased

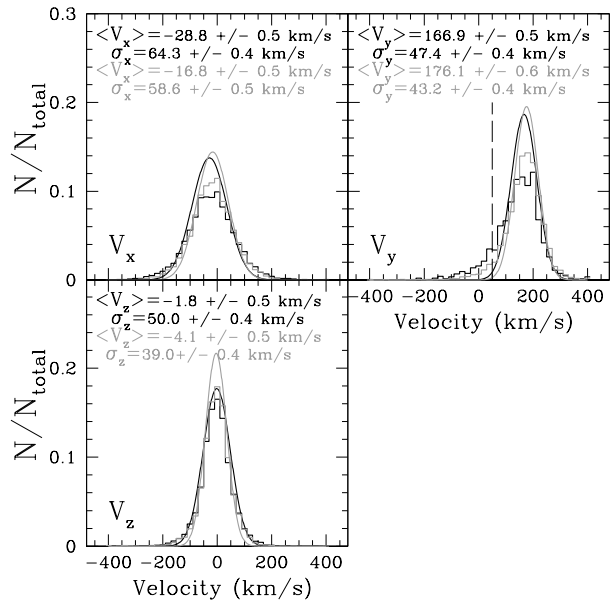


Figure 5. Velocity distributions of the thick disc sample using the distances of Zwitter et al. (2010) (black) and the clump thick disc sample (gray). The mean velocity values and dispersions (calculated using robust estimation) after removing stars with $V_y < 50 \text{ km s}^{-1}$ are given in each panel. The Gaussians plotted have the same mean and dispersion as the data.

amount of higher eccentricity stars was noticeable. These trends are natural consequences of increased contamination by halo stars. Overall, the higher $|z|$ distribution retained the general properties of the original distribution. Thus we conclude that the thin disc contamination is not likely to have a large effect on the overall shape of the eccentricity distribution.

3.2.3 Comparison of the original eccentricity distribution with those using different thick disc samples

Since the distances are a key component in calculating the eccentricity distribution, we also used another set of distances. Zwitter et al. (2010) calculated distances for a RAVE data set (based on a later internal data release consisting of 332,747 stars) by means of a photometric parallax method based on that of Breddels et al. (2010) but using the Y^2 , Dartmouth (Dotter et al. 2008), and Padova isochrones uniformly, rather than logarithmically spaced in time and, when picking a best match model star, weighting the model star picked based on mass. No age constraint to tailor the distances to a thick disc sample was applied in this set of distances. Using the same cleaning and thick disc selection criteria as before, we selected a sample from this catalogue (that based on the Y^2 isochrones) and calculated its eccentricity distribution. This thick disc sample consists of 6173 stars. See Figure 5 for the velocity distributions.

In order to have a more independent check on the eccentricity distribution, since the above two methods of calculating distances are quite similar, we selected a thick disc

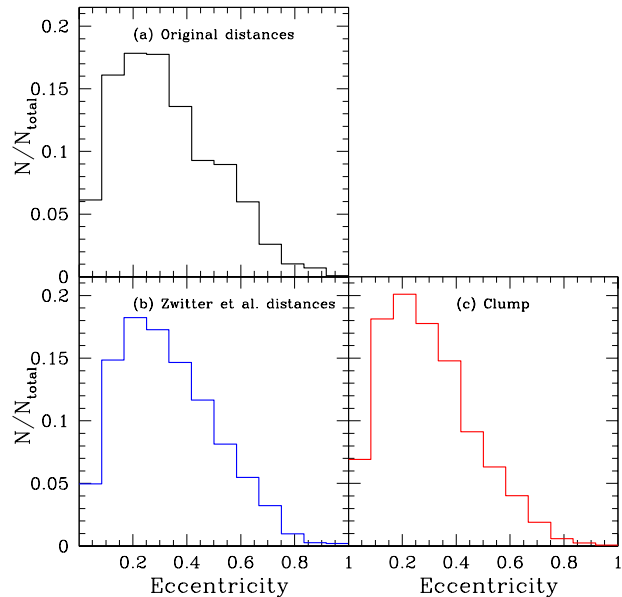


Figure 6. Eccentricity distributions of thick disc samples using a) the original distances, b) the Zwitter et al. distances, and c) the clump sample.

sample of clump stars from RAVE. To choose this sample, we used the same cleaning criteria on the full data release but did not impose the restrictions aimed at eliminating the clump stars. We identified the clump by colour and gravity, taking it to have $0.6 < J - K_s < 0.7$ and $1.5 < \log(g) < 2.7$. Then, we calculated the distances using the apparent magnitudes and assuming an absolute clump magnitude of $M_K = -1.61$, as in Alves & Sarajedini (1999). Finally, we imposed the same restrictions in $|z|$, volume, and velocity as before and calculated the eccentricity distribution. The resulting sample includes 3573 stars, and the velocity distributions are given in Figure 5.

The velocity distributions in Figure 5 show good agreement with those based on the Breddels et al. (2010) distances. As expected, the velocity dispersions for the red clump sample are slightly lower, since this sample should be devoid of halo contamination (as red clump stars are only present in young or intermediate age populations). Figure 6 shows that also the thick disc eccentricity distributions agree well with each other. All are strongly peaked at low eccentricities, have a generally triangular shape, and do not have a secondary peak at high eccentricity. The sample based on Breddels et al. (2010) falls off at high eccentricities less smoothly than the other two, but that could be due to statistical fluctuations in this much smaller data set. On the other hand, the clump sample has its peak at a lower eccentricity and contains a smaller number of stars at higher eccentricities as expected since this region is populated mainly by halo stars which are only present in the red giant samples. So while the three distributions are not identical, they agree fairly closely. Results of the application of KS tests show that all three are consistent with being drawn from the same distribution. This leads us to conclude that the eccentricity distribution is reasonably robust to the exact thick disc sample selection.

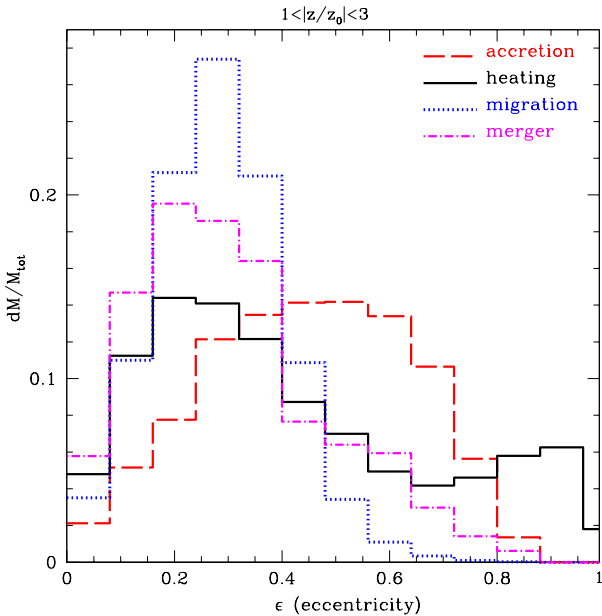


Figure 7. Comparison of the eccentricity distributions of each thick disc formation model for stars in the range 1–3 (thick disc) scale-heights and cylindrical distance $2 < R/R_d < 3$.

4 COMPARISON WITH THEORETICAL MODELS

4.1 Discussion of the models

We now compare our calculated eccentricity distribution to those computed by Sales et al. (2009) from the simulations of Abadi et al. (2003), Villalobos & Helmi (2008), Roškar et al. (2008), and Brook et al. (2004). These simulations have been discussed in the literature, so we will only briefly describe them here. For details, we refer the reader to the literature and to Table 1 of Sales et al. (2009), which summarises their main parameters.

Abadi et al. (2003) demonstrate the formation of the thick disc through accretion of satellites during the hierarchical formation of a Milky Way-like galaxy in the Λ cold dark matter paradigm and using cosmological N -body/smoothed particle hydrodynamics (SPH) simulations.

In the heating scenario simulation of Villalobos & Helmi (2009), a satellite merges with a primary thin disc (of comparable mass) on a prograde orbit inclined 30 degrees. The subsequent formation of a new thin disc from cooling gas and any changes that might cause in the thick disc were not modelled in this simulation.

The simulation of Roškar et al. (2008) models the formation of a galactic disc by starting with a dark matter halo and a hot gas halo which over 10 Gyrs cools and forms stars in a disc which migrate as transient spiral structure forms.

Brook et al. (2004) model the formation of a disc in a semi-cosmological N -body/SPH simulation which incorporates gas heating and cooling, star formation, feedback, and chemical enrichment. Their thick disc develops during gas rich mergers.

Sales et al. (2009) found that the location of the peak and the shape of the eccentricity distributions are driven by what kind of stars make up the thick disc in each model, as shown in Figure 7. In the accretion scenario, the thick disc is composed mostly of accreted material; since satellites tend to be on radial orbits, the resulting eccentricity distribution is relatively broad and peaks in the mid to high eccentricities. The other three scenarios involve a thick disc being composed primarily from stars formed *in situ*. Such stars have more circular orbits, which produce a peak at low values of the eccentricity. The heating and the gas-rich merger simulations have a contribution of accreted stars to the thick disc, which show up in the eccentricity distribution as a distinct second but much smaller peak at high eccentricity in the heating scenario and a lumpiness at mid to high eccentricities in the merger case.

4.2 Comparison with the models

Comparison of Figures 6 and 7 shows that the eccentricity distribution of our sample does not support the accretion model. The triangular shape with a peak at low eccentricities of our distribution does not resemble the broad mound peaked at middling eccentricity that characterises the accretion scenario. The eccentricity distribution of our thick disc sample with its prominent peak at low eccentricities is consistent with the distribution displayed by the heating, migration, and merger scenarios. Our distribution does not exhibit a secondary peak at high eccentricities like that evident in the heating model due to the accreted satellite. However, the location of this secondary peak depends on the initial orbital configuration of the accreted satellite. If the initial conditions were changed to produce a secondary peak at middling eccentricities this could probably be obscured in the data by the larger fraction of *in situ* stars.

While the distributions from the migration and merger models are not identical to the distribution of our sample, they do show some resemblance and have no features that seem to count against either being possible. The gas-rich merger's distribution even displays an asymmetric peak like our distribution, making this scenario the most consistent with our data. The migration distribution exhibits a symmetry about the peak (is more Gaussian-like) until it gets down into the high eccentricity tail that is not displayed in our distribution, making the migration scenario somewhat less consistent with our data.

There are several reasons for the models not being a perfect match to the data. Random and systematic errors in the data, while not significantly affecting the overall characteristics of the distribution, can alter the exact shape, especially at high eccentricities. Also, since the simulations did not attempt to duplicate the Milky Way exactly, they might not be similar enough to the Galaxy to precisely mimic the eccentricity distribution even if the formation mechanism is correct. It is also plausible that the thick disc was formed by a combination of processes. Radial migration has been shown to be dynamically possible in a galaxy such as our own; mergers, including gas-rich, are known to occur. Thus, the nature of the measured eccentricity distribution could be indicating that both radial migration and gas-rich mergers contributed to its formation.

One possible way to investigate which model is the most

likely, would be to compute the eccentricity distributions of the models and the data for different locations along the Galactic disc, as one may expect the contribution of accreted populations to change with distance and become more dominant in the Galaxy's outskirts. Undoubtedly, data from *Gaia* when it becomes available will aid in clarifying how exactly the Galactic thick disc formed.

5 SUMMARY AND CONCLUSIONS

We have isolated a sample of thick disc stars from RAVE survey data, calculated its eccentricity distribution, and determined that the distribution is fairly robust to changes in distances, thin disc contamination, and the specific thick disc sample used. Our eccentricity distribution is fairly triangular in shape, depicting a dominant peak at low eccentricity and a relatively smooth falloff at high values.

We have compared this finding with the eccentricity distributions in Sales et al. (2009) presented for simulated thick discs formed via accretion, heating via a minor merger, radial migration, and gas-rich mergers. The broad peak at moderately high eccentricities of the accretion model is not consistent with the relatively narrow peak at low eccentricity displayed by our sample. This indicates that the Galactic thick disc formed predominantly *in situ*. A lack of a distinguishable secondary peak at high eccentricity further suggests that if any of the thick disc was accreted, its direct contribution of stars in the Solar neighbourhood was minimal. The gas-rich mergers simulation, and to a somewhat lesser extent, the radial migration model, are consistent with the distribution of our sample. This suggests that these formation mechanisms could have had some role in the formation of the Milky Way's thick disc.

ACKNOWLEDGEMENTS

We are indebted to Laura V. Sales for producing Figure 7 of this Paper. AH acknowledges financial support from the European Research Council under ERC-Starting Grant GALACTICA-240271. HLM has been supported by the NSF through grant AST-0098435.

Funding for RAVE has been provided by the Anglo-Australian Observatory, the Astrophysical Institute Potsdam, the Australian Research Council, the German Research Foundation, the National Institute for Astrophysics at Padova, The Johns Hopkins University, the Netherlands Research School for Astronomy, the Natural Sciences and Engineering Research Council of Canada, the Slovenian Research Agency, the Swiss National Science Foundation, the National Science Foundation of the USA (AST-0508996), the Netherlands Organisation for Scientific Research, the Particle Physics and Astronomy Research Council of the UK, Opticon, Strasbourg Observatory, and the Universities of Basel, Cambridge, and Groningen. The RAVE Web site is at www.rave-survey.org.

REFERENCES

- Abadi M. G., Navarro J. F., Steinmetz M., Eke V. R., 2003, *ApJ*, 597, 21

- Alves D. R., Sarajedini A., 1999, *ApJ*, 511, 225
Bournaud, F., Elmegreen, B. G., & Martig, M. 2009, *ApJ*, 707, L1
Breddels M. A., et al., 2010, *A&A*, 511, A90
Brook C. B., Kawata D., Gibson B. K., Freeman K. C., 2004, *ApJ*, 612, 894
Burstein D., 1979, *ApJ*, 234, 829
Chabrier G., 2001, *ApJ*, 554, 1274
Demarque P., Woo J.-H., Kim Y.-C., Yi S. K., 2004, *ApJS*, 155, 667
Dotter A., Chaboyer B., Jevremović D., Kostov V., Baron E., Ferguson J. W., 2008, *ApJS*, 178, 89
Edvardsson B., Andersen J., Gustafsson B., Lambert D. L., Nissen P. E., Tomkin J., 1993, *A&A*, 275, 101
Gilmore G., Reid N., 1983, *MNRAS*, 202, 1025
Hernquist L., 1990, *ApJ*, 356, 359
Kregel M., van der Kruit P. C., Freeman K. C., 2005, *MNRAS*, 358, 503
Marigo P., Girardi L., Bressan A., Groenewegen M. A. T., Silva L., Granato G. L., 2008, *A&A*, 482, 883
Minchev, I., & Famaey, B. 2009, arXiv:0911.1794
Miyamoto M., Nagai R., 1975, *PASJ*, 27, 533
Roškar R., Debattista V. P., Stinson G. S., Quinn T. R., Kaufmann T., Wadsley J., 2008, *ApJ*, 675, L65
Sales L. V., et al., 2009, *MNRAS*, L336
Schönrich R., Binney J., 2009, *MNRAS*, 399, 1145
Sellwood J. A., Binney J. J., 2002, *MNRAS*, 336, 785
Sparke L. S., Gallagher J. S., III 2006, *Galaxies in the Universe - 2nd Edition*, Cambridge University Press
Steinmetz M., et al., 2006, *AJ*, 132, 1645
van der Kruit P. C., Searle L., 1981, *A&A*, 95, 105
VandenBerg D. A., Gustafsson B., Edvardsson B., Eriksson K., Ferguson J., 2007, *ApJ*, 666, L105
Veltz L., et al., 2008, *A&A*, 480, 753
Villalobos Á., Helmi A., 2008, *MNRAS*, 391, 1806
Villalobos Á., Helmi A., 2009, *MNRAS*, 399, 166
Yanny B., et al., 2009, *AJ*, 137, 4377
Yoachim P., Dalcanton J. J., 2006, *AJ*, 131, 226
Yoshii Y., 1982, *PASJ*, 34, 365
Zwitter T., Siebert A., Munari U., et al., 2008, *AJ*, 136, 421
Zwitter T., et al., 2010, arXiv:1007.4411

This paper has been typeset from a \TeX / \LaTeX file prepared by the author.